

Two-dimensional SPH simulation of liquid sloshing in a rotating tank

J.R. Shao¹, †M.B. Liu²

¹College of Mechanical Engineering, Chongqing University of Technology, Chongqing, China

²College of Engineering, Institute of Ocean Research, State Key Laboratory for Turbulence and Complex systems, Peking University, Beijing, China

† Corresponding author: mbliu@pku.edu.cn

Abstract

This paper presents the application of an improved smoothed particle hydrodynamics (SPH) method to simulate violent liquid sloshing in a rotating liquid tank. The dynamic response of the sloshing system and the change of the pressure profiles are investigated in detail while the SPH simulations are conducted under different external excitations and different water waves. It is revealed that for small amplitude liquid sloshing, the linear wave theory can apply and free surface does not break up. For liquid sloshing with strong nonlinear effects, free surface evolves violently with breakup and impinging onto bulky water and solid walls, and therefore the linear wave theory is no longer valid. A circular frequency deviated from the natural frequency from linear wave theory may produce bigger maximal pressure load than the case with equivalent natural frequency.

Keywords: SPH, liquid sloshing, dynamic response, circular frequency

1. Introduction

Sloshing refers to the movement of liquid inside a partially-filled container due to external excitations. As a complex hydrodynamic phenomenon, liquid sloshing involves the change of free surfaces and the strong coupling between liquid and containers, which are usually thin-shelled structures. Liquid sloshing can be frequently observed in daily life, engineering and sciences. When the amplitude of an external excitation is very large or its frequency is close to the natural frequency of the liquid sloshing system, the liquid inside the container can exhibit violent oscillations, and exert strong impact load on the container[1]. For example, large liquid sloshing in an oil or liquefied natural gas ship may result in local breakages and global instability to the ship, and further lead to leakage of oil, and capsizing of ship. The sloshing of liquefied fuel inside the fuel tank in an aeronautic or astronautic craft can disturb or even breakdown normal navigation of the craft.

Liquid sloshing has been a hot research subject attracting much attention over the last decades. The majority of theoretical publications are restricted to linear theory associated with non-resonant excitation and small forcing magnitude[2-5]. There are also some works based on weakly nonlinear semi-analytical theories, which used the assumptions that an inviscid incompressible liquid is in irrotational flow, the liquid surface does not overturn or break, and the surface tension does not matter [6-8]. All these theories in general, may result in big errors in the time-history response when the external excitation is large or near the natural frequency. Recently more and more researches on liquid sloshing are focused on numerical simulations with the advancement of the computer techniques [9-11]. However, most of the numerical simulations are focused on grid-based methods, such as FDM [12, 13], FEM [14, 15] and BEM [16-19]. Liquid sloshing is a complex fluid motion, which usually involves changing and breakup of free surfaces, strong turbulence and vortex, and violent fluid-solid interaction. Traditional grid-based numerical methods have difficulties in tracking changing free surfaces or moving interfaces, and usually need mesh adjustment or rezoning [20-22].

The meshfree and particle methods provide new alternates for investigating liquid sloshing problems [23, 24]. Among these methods, smoothed particle hydrodynamics (SPH) [25-27] combines the advantages of meshfree, Lagrangian and particle methods. In SPH, particles are used to represent the state of a system and these particles can freely move according to internal particle interactions and external forces. Therefore it can naturally obtain history of fluid motion, and can easily track material interfaces, free surfaces and moving boundaries. There are a few literatures addressing the application of SPH method to liquid sloshing dynamics. For example, Delorme et al. simulated the sloshing loads in LNG tankers with SPH [28]. Iglesias et al. simulated the anti-roll tanks and sloshing type problems[29]. Rhee and Engineer studied liquid tank sloshing with Reynolds-averaged Navier-Stokes[30]. Souto-Iglesias et al. assessed the liquid moment amplitude in sloshing type problems with smooth particle hydrodynamics[31]. Anghileri investigated the fluid-structure interaction of water filled tanks during the impact with the ground[32]. These works have demonstrated the feasibility of SPH method in modeling liquid sloshing dynamics. However, previous works are generally based on traditional SPH method, which have poor computational accuracy, and it is hard to track the variations of pressure. In this paper, an improved SPH model is used to simulate the liquid sloshing in a rotating tank.

2. SPH methodology

The governing motion of liquid sloshing in isothermal condition can be described by the following continuity and momentum equations

$$\frac{d\rho}{dt} = -\rho \nabla \cdot \mathbf{v}, \quad (1)$$

$$\frac{d\mathbf{v}}{dt} = -\frac{1}{\rho} \nabla P + \frac{\mu}{\rho} \nabla^2 \mathbf{v} + \mathbf{g} + \frac{1}{\rho} \bar{\nabla}(\rho \mathbf{R}), \quad (2)$$

where ρ is fluid density, \mathbf{v} is the velocity vector, P is pressure, μ is the dynamic viscosity, \mathbf{g} is the gravitational acceleration, and \mathbf{R} is the Reynolds stress tensor. The eddy viscosity assumption is used to model the Reynolds stress tensor as:

$$\mathbf{R} = 2\nu_t \mathbf{S} - \frac{2}{3} k \mathbf{I}, \quad (3)$$

where ν_t is the eddy viscosity, \mathbf{S} is the mean rate-of-strain tensor, k is turbulence kinetic energy and \mathbf{I} is a unit tensor. The Smagorinsky model of eddy viscosity $\nu_t = (C_s \Delta l)^2 \sqrt{2S_{ij}S_{ij}}$ is widely used, where C_s is the Smagorinsky constant usually taken as 0.12 and Δl is a mixing length which is assumed to be the initial particle spacing in SPH. S_{ij} is the elements of \mathbf{S} given by:

$$S_{ij} = \frac{1}{2} \left(\frac{\partial v_j}{\partial x_i} + \frac{\partial v_i}{\partial x_j} \right). \quad (4)$$

Considering $k = \overline{v_i'v_j'}/2$ and $R_{ij} = -\overline{v_i'v_j'}$, the relation between k and the Reynolds stress tensor can be written as $k = -R_{ii}/2$.

In SPH, the state of a system is represented by a set of particles, and flow field variables (such as density, velocity, acceleration) can be obtained through approximating the governing

equations which are discretized on the set of particles. A field function and its derivative can then be written in the following forms

$$\langle f(\mathbf{x}_i) \rangle = \sum_{j=1}^N \frac{m_j}{\rho_j} f(\mathbf{x}_j) W(\mathbf{x}_i - \mathbf{x}_j, h), \quad (5)$$

$$\langle \nabla \cdot f(\mathbf{x}_i) \rangle = \sum_{j=1}^N \frac{m_j}{\rho_j} f(\mathbf{x}_j) \nabla_i W_{ij}, \quad (6)$$

where $\langle f(\mathbf{x}_i) \rangle$ is the approximated value of particle i ; $f(\mathbf{x}_j)$ is the value of $f(\mathbf{x})$ associated with particle j ; \mathbf{x}_i and \mathbf{x}_j are the positions of corresponding particles; m denotes mass; h is the smooth length; N is the number of the particles in the support domain; W is the smoothing function representing a weighted contribution of particle j to particle i . The cubic spline function has continuous second-order derivative, and it is not sensitive to particle disorder. It is given by

$$W(R, h) = a_d \times \begin{cases} 1 - \frac{3}{2}R^2 + \frac{3}{4}R^3, & 0 \leq R < 1 \\ \frac{1}{4}(2-R)^3, & 1 \leq R < 2 \\ 0, & R \geq 2 \end{cases} \quad (7)$$

where a_d is $3/2h$, $10/7\pi h^2$ and $1/\pi h^3$ in one-, two- and three-dimensional space, respectively, so that the condition of unity can be satisfied for all the three dimensions. $R = |\mathbf{x} - \mathbf{x}'|/h$.

Through particle approximation, the governing motion of fluid flow in isothermal condition can be described by the following continuity and momentum equations

$$\frac{d\rho_i}{dt} = \sum_{j=1}^N m_j \mathbf{v}_{ij} \cdot \nabla_i W_{ij}, \quad (8)$$

$$\begin{aligned} \frac{d\mathbf{v}_i}{dt} = & - \sum_{j=1}^N m_j \left(\frac{p_i}{\rho_i^2} + \frac{p_j}{\rho_j^2} \right) \cdot \nabla_i W_{ij} + \sum_{j=1}^N \frac{4m_j (\mu_i + \mu_j) \mathbf{x}_{ij} \cdot \nabla_i W_{ij}}{(\rho_i + \rho_j)^2 (x_{ij}^2 + 0.01h^2)} \mathbf{v}_{ij} \\ & + \sum_b m_b \left(\frac{\mathbf{R}_a}{\rho_a} + \frac{\mathbf{R}_b}{\rho_b} \right) \cdot \nabla_a W_{ab} + \mathbf{g} \end{aligned} \quad (9)$$

To solve the equations of motion, an artificial compressibility technique is usually used to model the incompressible flow as a slightly compressible flow. Therefore, it is feasible to use a quasi-incompressible equation of state to model the incompressible flow. A commonly used artificial equation of state is

$$P = C_0^2 (\rho - \rho_0), \quad (10)$$

where ρ_0 is the reference density, and it is taken as the initial density of the water. C_0 is the sound speed.

It is known that the conventional SPH method has been hindered with low accuracy as it cannot exactly reproduce quadratic and linear functions, and even cannot exactly reproduce a

constant. The accuracy is also closely related to the distribution of particles, selection of smoothing function and the support domain (described by the smoothing length h multiplied by a scalar factor). In liquid sloshing problem, the changing and breakup of free surfaces as well as splashing and fall of water particles lead to highly disordered particle distribution, which can seriously influence computational accuracy of SPH approximations. Therefore improving the particle inconsistency and hence the approximation accuracy is necessary. In this work, the KGC model[33] for approximating kernel gradient is used. It is obtained based on Taylor series expansion on the SPH approximation of a function, and can guarantee the second order accuracy in the whole computational domain. It is given by

$$\nabla_i^C W_{ij} = L(\mathbf{r}_i) \nabla_i W_{ij}, \quad (11)$$

$$L(\mathbf{r}_i) = \left(\sum_j \begin{pmatrix} x_{ji} \frac{\partial W_{ij}}{\partial x_i} & y_{ji} \frac{\partial W_{ij}}{\partial x_i} \\ x_{ji} \frac{\partial W_{ij}}{\partial y_i} & y_{ji} \frac{\partial W_{ij}}{\partial y_i} \end{pmatrix} V_j \right)^{-1}. \quad (12)$$

It is noted that, the new kernel gradients are obtain after searching particles, and then they can be used for the approximation of and field variables, therefore it can save a lot of computing time. And there is no need to significantly change the structure of SPH computer programs and procedure of SPH simulations.

In SPH, solid boundary conditions are not able to be directly and rigorously implemented as in the grid-based numerical models. In this work, a coupled dynamic solid boundary treatment algorithm(SBT) [34] (Fig.1) is used to construct the solid boundary, which can predict the pressure of the solid boundary accurately.

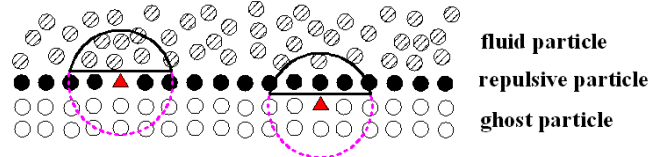


Figure 1. Illustration of the coupled dynamic SBT algorithm.

In this coupled dynamic SBT algorithm, the information of repulsive particles only comes from fluid particles, and the information of ghost particles comes from both fluid and repulsive particles. For non-slip boundary condition, variables of the boundary particles (both repulsive and ghost particles) can be obtained as follows,

$$\rho_i^{new} = \sum_{j=1}^N \rho_j W_{ij}^{new} \frac{m_j}{\rho_j} = \sum_{j=1}^N m_j W_{ij}^{new}, \quad (13)$$

$$v_i = - \sum_{j=1}^N v_j W_{ij}^{new} \frac{m_j}{\rho_j}, \quad (14)$$

$$W_{ij}^{new} = \frac{W_{ij}}{\sum_{j=1}^N W_{ij} \frac{m_j}{\rho_j}}. \quad (15)$$

For particles near the free surface, the support domains are usually cut off, and the kernel function do not keep the normalized nature. It has great influence to particle approximation. To resolve the problem, a simple but very effective treatment is presented, which is obtained based on interpolation of kernel function,

$$k_i = \sum_{j=1}^N W_{ij} \frac{m_j}{\rho_j} \leq 0.9 . \quad (16)$$

Here, k_i is a coefficient, it is calculated each time step. If the value is less than 0.9, it is considered to be the free surface particle, and the pressure will be equal to atmospheric pressure, its density is equal to the initial value.

3. SPH modelling of sloshing in a rotating liquid tank

In this section, the liquid sloshing in a rotating tank is investigated under different external excitations. Fig. 2 shows the geometry of the liquid sloshing system, which is similar to what Iglesias provided [31]. i.e., $L=0.64$ m, $H=1.15$ m, the water depth is $h_w=0.03$ m, and the centre of rotation is 0.1 m below the baseline.

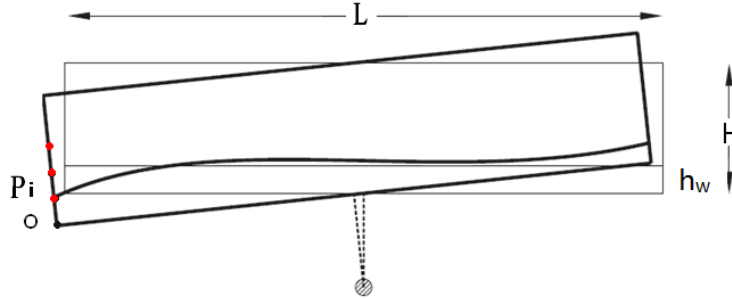


Figure 2. Illustration of liquid sloshing in a rotating tank.

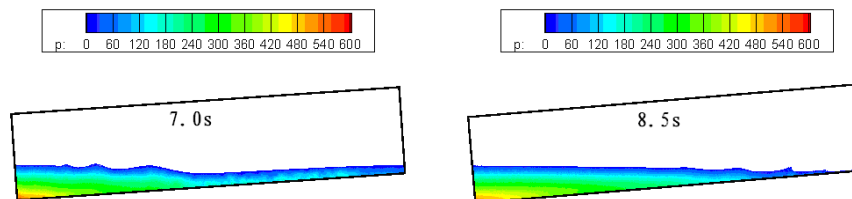
The external excitation can be described as $\theta = \theta_0 \sin(\omega t)$, where θ_0 is the angular displacement, ω is the circular frequency of the rotating motion. In the left wall, eight probe points P1-P8 are employed, $OP1 = P1P2 = \dots = P7P8 = 0.01$ m. In this model, the water depth is very small comparing with the size of the tank, therefore the corresponding first resonance frequency can be obtained from the linear wave theory[31],

$$\omega = \sqrt{\frac{g\pi}{L} \tanh\left(\frac{\pi h_w}{L}\right)}. \quad (17)$$

Therefore, the value of the first resonance frequency is 2.65 rad/s.

3.1 Liquid sloshing under different circular frequencies

To investigate the free surface evolution and the pressure load on the tank under different circular frequencies, the sloshing models are set as $\theta_0 = 6^\circ$, and $\omega = 1.0, 2.65, 4.34, 8.21$ rad/s respectively.



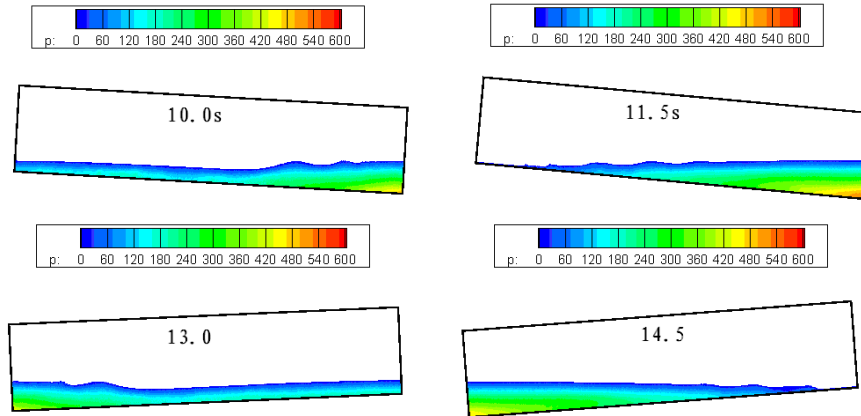


Figure 3. Pressure field with $\omega=1.0$ rad/s.

When $\omega = 1.0$ rad/s, the period of the external excitation is 6.28s. Fig.3 shows the corresponding liquid sloshing mode and free surface evolution of the liquid sloshing system in a period. In this case, the frequency of the external excitation (1.0 rad/s) is less than the natural frequency (2.65 rad/s) and the free surface does not break up. Though there are nonlinear phenomena, the linear wave theory still applies. In the whole process of the sloshing, the water waves are travelling waves. Fig.4 is the pressure history at P3. It shows that the water impact the solid wall periodically, with an amplitude about 380 Pa.

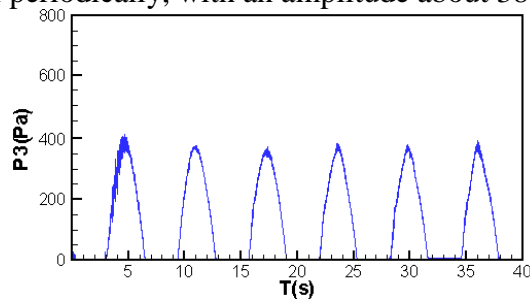


Figure 4. Pressure values at P3, $\omega=1.0$ rad/s.

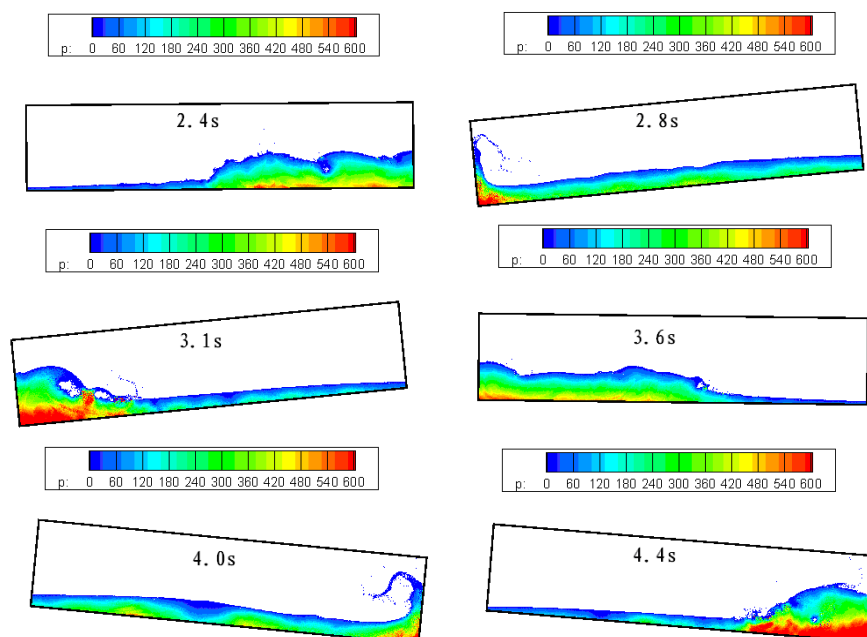


Figure 5. Pressure field with $\omega=2.65$ rad/s.

Next, we increase the value of ω to 2.65 rad/s, which equals to the natural frequency of sloshing system. The free surface evolution as well as the pressure field distribution is shown on Fig.5. Comparing Fig.5 with Fig.3, it is found that, liquid sloshing in this case is more violent with free surface break up. It can also be observed that with the development of the liquid sloshing, the water column impacts brutally against the solid wall, generates a bounce-back flow pattern after a short period of interaction with the vertical wall, and finally forms some cavities. The cavities change their shapes and disappear finally. The water wave is breaking wave and the linear wave theory may not be valid. Fig.6 shows that water exerts strong impact load on the solid wall (left and right wall) periodically, and the pressure amplitude is about 800 Pa at P3, which is much bigger than that in the above case.

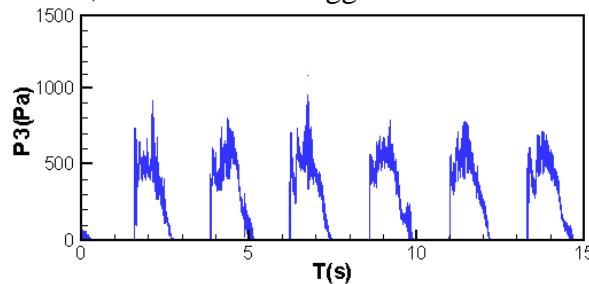
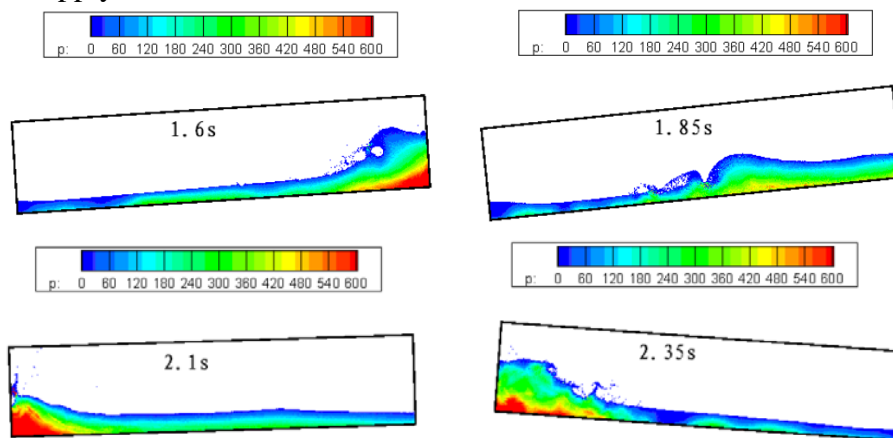


Figure 6. Pressure values at P3, $\omega=2.65$ rad/s.

Increasing the value of ω to 4.34 rad/s, the moving condition in Fig.7 can be obtained. The sloshing is still violent and the water wave has two main wave peaks. The front one is higher than the later one. These two surge fronts with two water wave peaks then impact the solid wall (left and right wall) twice, as shown in Fig. 8. The first impact is more violent with an instantaneous pressure peak (about 1200-1400 Pa). The pressure peak of the second impact is about 700-1000Pa. One notable observation is that in this case, the strongest wave impact can happen on the left-top and right-top corners. Also for this case, though the circular frequency is away from the first natural frequency (2.65 rad/), the maximal impact pressure values both for the first and second water impacts are bigger than the above case in which the circular frequency equals to the natural frequency. This is because the liquid sloshing is associated with strong nonlinear effects (with breaking free surface and violent water slamming on the solid wall & on the bulky water). For such highly nonlinear liquid sloshing, the linear wave theory does not apply.



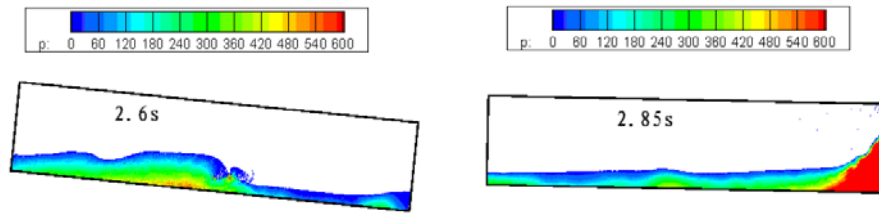


Figure 7. Pressure field with $\omega = 4.34$ rad/s.

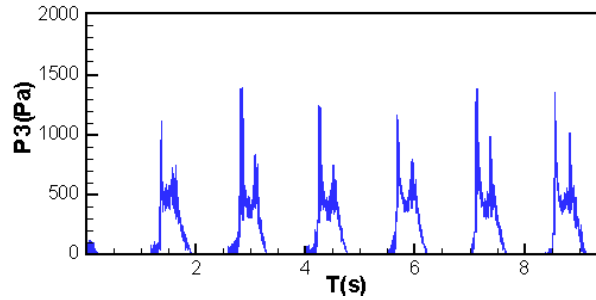


Figure 8. Pressure values at P3 with $\omega = 4.34$ rad/s.

Increasing the frequency of the external excitation to 8.21 rad/s, the amplitude of the liquid sloshing is much smaller than that in Fig.5. It is noted that as the frequency of the external excitation is so big, the movement of water is not able to follow the movement of the container. Free surface does not break up and the water wave becomes travelling wave again. Two and even more wave peaks occurs during the sloshing process (see Fig. 9) At the same time, the pressure peak will also decrease, as shown in Fig. 10, its value is about 250- 600Pa, and is different in different periods due to the interaction of different wave surge fronts.

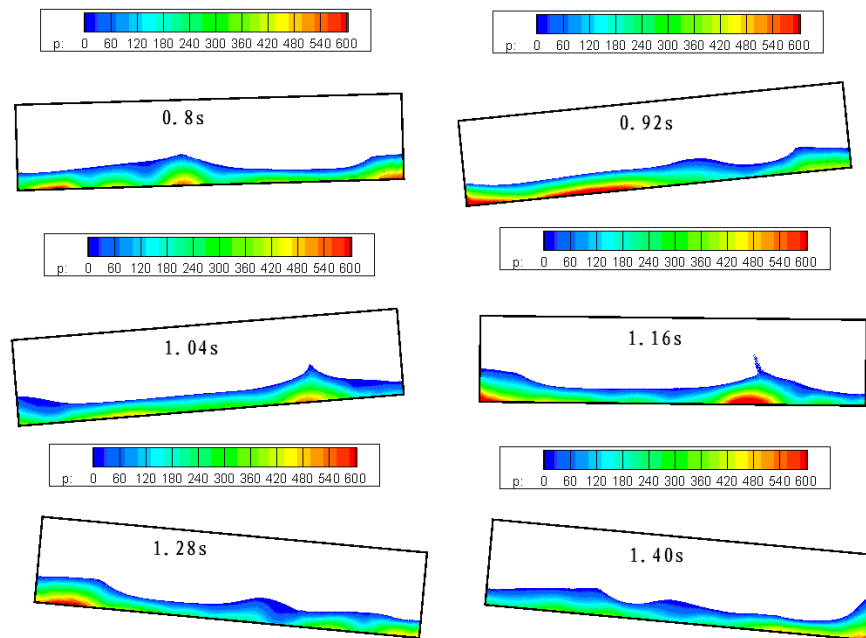


Figure 9. Pressure field with $\omega = 8.21$ rad/s.

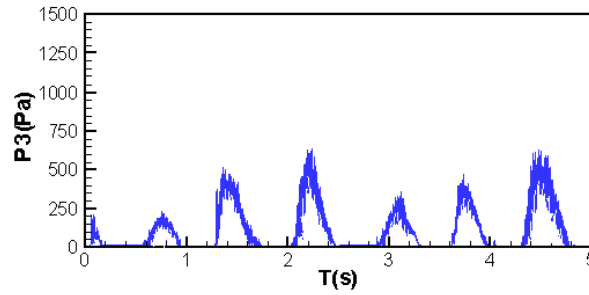


Figure 10. Pressure values at P3, $\omega=8.21$ rad/s.

3.2 Liquid sloshing under different angular displacements

To investigate the change of the free surface evolution, and the pressure load on the tank under different angular displacement, the sloshing models are set $\omega = 2.65$ rad/s (corresponding to the natural frequency), $\theta_0 = 4^\circ, 6^\circ, 8^\circ, 10^\circ, 12^\circ$ separately. The liquid sloshing with $\theta_0 = 4^\circ$ can be observed in Fig.10. Comparing the pressure field with Fig.5 ($\theta_0 = 6^\circ$) and Fig.11 ($\theta_0 = 10^\circ$), it is found that the amplitude of the sloshing increase with the increasing of the angular displacement.

Fig.12 shows the pressure curves in the eight probes with $\theta_0 = 4^\circ$. The peak values of the pressure change from 180 Pa to 950 Pa. When the angular displacement adds up to 10° , free surface breaks up and the water wave becomes rougher and the whole flow domain involves strong turbulence and vortex. To describe the turbulence more accurately, the RANS turbulence model is necessary. Fig.13 shows the evolution of the cavities in the flow domain. The water column impacts brutally against the solid wall. When $t = 6.3$ s, the water front impacted on the top of the container, and generated a bounce-back flow pattern. Fig. 14 shows that the peak values of the pressure change from 400Pa to 1400 Pa, which is bigger than that when $\theta_0 = 4^\circ$. For a specific angular displacement at natural frequency, the pressure load on the right or left solid wall will reduce with the increase of the height of the observation points.

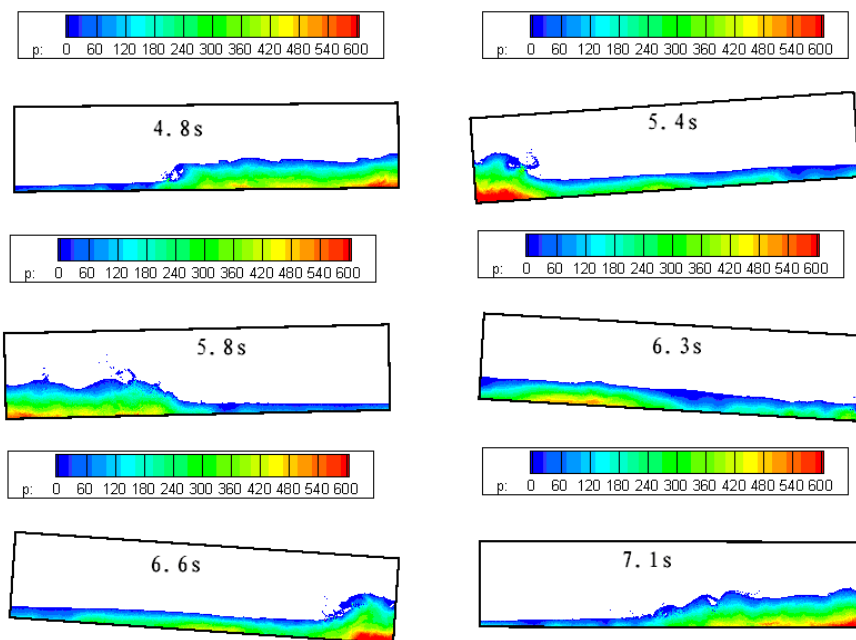


Figure 11. Pressure field with $\theta_0 = 4^\circ$, $\omega = 2.65\text{rad/s}$

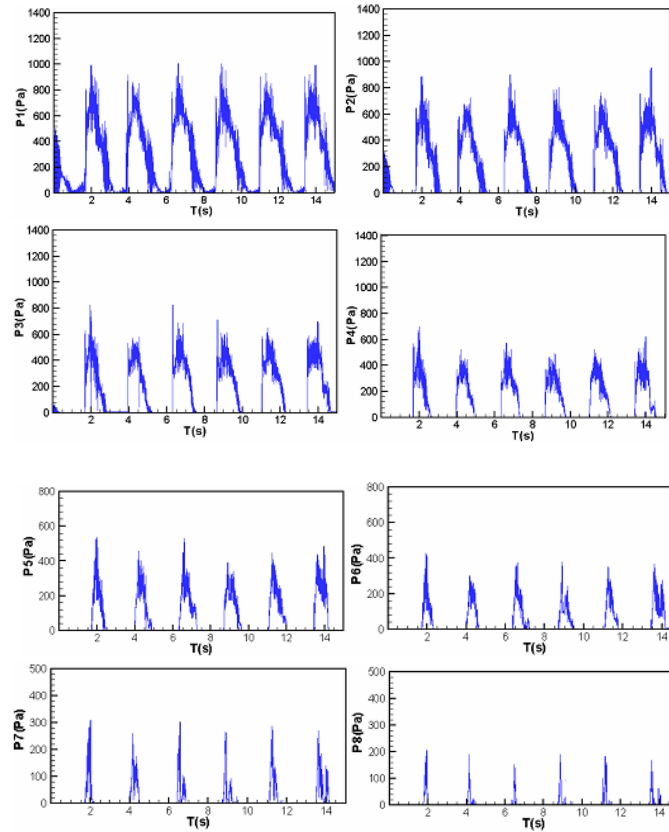


Figure 12. Pressure values at P1-P8, $\theta_0 = 4^\circ$

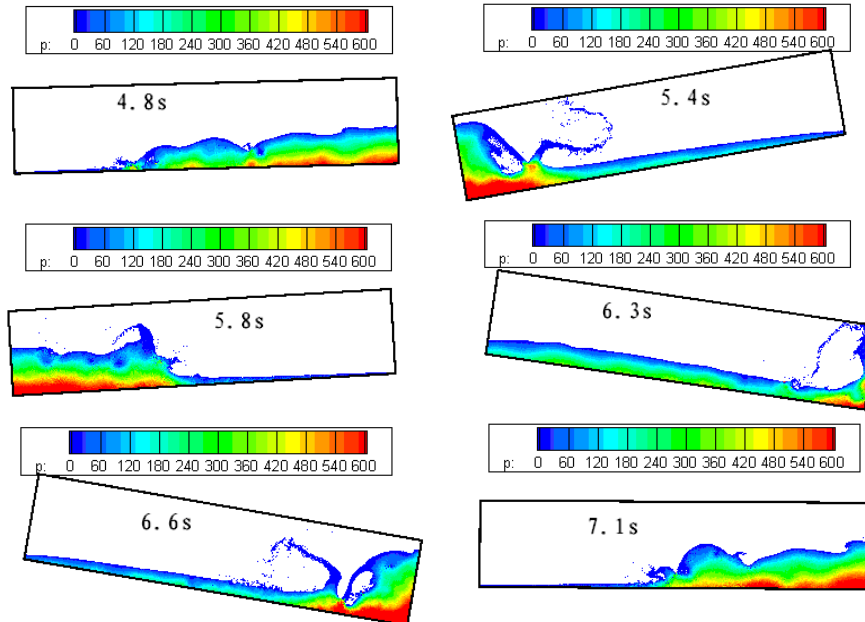


Figure 13. Pressure field with $\theta_0 = 10^\circ$, $\omega = 2.65\text{ rad/s}$.

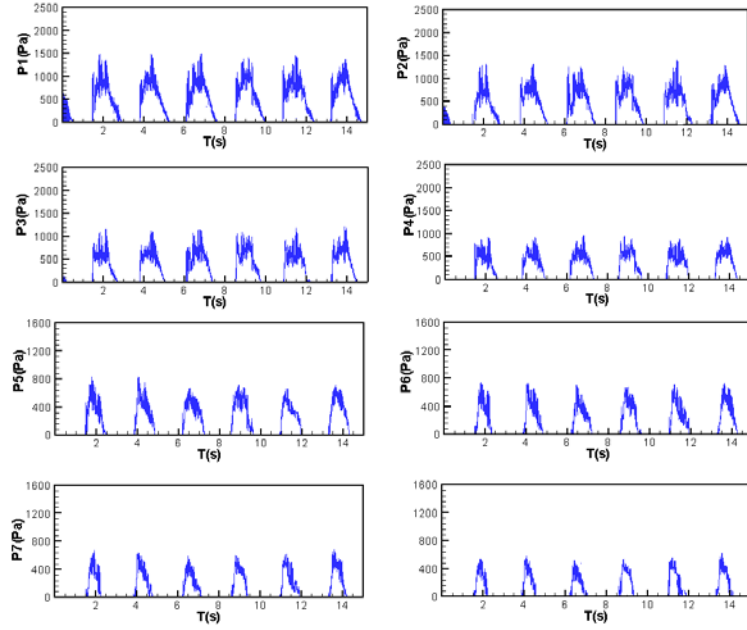


Figure 14. Pressure values at P1-P8, $\theta_0 = 10^\circ$.

Conclusions

In this paper, an improved SPH model is used for the simulation of liquid sloshing in a rotating tank which moves under different external excitations. The KGC and density correction can improve the computational accuracy and obtain smoothed pressure field; the coupled dynamic solid boundary treatment can remove the numerical oscillation near the solid boundary and ensure no penetration condition.

From the numerical simulations, the following conclusions can be drawn:

- 1) The liquid inside the container can demonstrate different sloshing behaviours with different circular frequency. For small circular frequencies, liquid sloshing is associated with smoothly evolving free surface and the linear wave theory is valid. The resultant water wave behaves as traveling waves and the maximal impact pressure happens on the left and right walls of the container.
- 2) For cases with circular frequencies close to or slightly bigger than the natural frequency, the sloshing liquid is highly nonlinear, and the linear wave theory is no longer valid. Therefore, the maximal pressure load obtained with the circular frequency equivalent to the natural frequency from linear wave theory may not necessary bigger than those from circular frequencies deviated from the natural frequency from linear wave theory.
- 3) For cases with very large circular frequencies, the movement of water is not able to follow the movement of the container. Free surface does not break up and the water wave becomes travelling waves again. Two and even more wave peaks may occur during the sloshing process.
- 4) Changing the angular displacement can also lead to different sloshing patterns. Increasing the angular displacement can lead to more violent movement. For a specific angular displacement at the natural frequency, the pressure load on the right or left solid wall will reduce with the increase of the height of the observation points.

Acknowledgement This work has been supported by the National Natural Science Foundation of China (11602045), NSAF (Grant No.U1530110), Natural Science Foundation of Chongqing (cstc2016jcyjA0373), STRPCMEC (Grant No.KJ1600918).

References

- [1] Ibrahim,R.A. (2005) Liquid sloshing dynamics: theory and applications, Cambridge University Press.
- [2] Karamanos, S.A., Patkas, L.A. and Platyrrachos, M.A. (2006) Sloshing effects on the seismic design of horizontal-cylindrical and spherical industrial vessels. *Journal of pressure vessel technology*, **128(3)**, 328-340.
- [3] Patkas, L.A. and Karamanos,S.A. (2007) Variational solutions for externally induced sloshing in horizontal-cylindrical and spherical vessels. *Journal of engineering mechanics*, **133(6)**, 641-655.
- [4] Drodos, G.C., Dimas, A.A, and Karabalis, D.L. (2008) Discrete modes for seismic analysis of liquid storage tanks of arbitrary shape and height. *J. Pressure Vessel Technology*, **130**, 0418011.
- [5] Hasheminejad, S.M. and Aghabeigi, M. (2009) Liquid sloshing in half-full horizontal elliptical tanks. *Journal of Sound and Vibration*, **324 (1)**, 332-349.
- [6] Gavriluk, I.P., Lukovsky, I.A. and Timokha, A.N. (2000) A multimodal approach to nonlinear sloshing in a circular cylindrical tank. 2000. *Hybrid Method Engng*, **2(4)**, 463-183.
- [7] Faltinsen, O.M., Rognebakke, O.F. and Timokha,A.N. (2003) Resonant three-dimensional nonlinear sloshing in a square-base basin. *Journal of Fluid Mechanics*, **487**, 1-42.
- [8] Gavriluk, I., Lukovsky, I., Trotsenko, Y. and Timokha, A. (2006) Sloshing in a vertical circular cylindrical tank with an annular baffle. Part 2. NonLinearresonant waves, *Journal of Engineering Mathematics*, **54(1)**, 71-88.
- [9] Ibrahim, R.A., Pilipchuk, V.N. and Ikeda, T. (2001) Recent advances in liquid sloshing dynamics. *Applied Mechanics Reviews*, **54**,133-199.
- [10]Faltinsen, O.M. and Timokha, A.N. (2009) Sloshing, Cambridge University Press.
- [11]Cariou, A. and Casella, G. (1999) Liquid sloshing in ship tanks: a comparative study of numerical simulation. *Marine structures*, **12(3)**, 183-198.
- [12]Chen, B.F. and Nokes, R. (2005) Time-independent finite difference analysis of fully non-linear and viscous fluid sloshing in a rectangular tank. *Journal of Computational Physics*, **209(1)**: 47-81.
- [13]Chen, B.F. (2005) Viscous fluid in tank under coupled surge, heave, and pitch motions. *Journal of waterway, port, coastal, and ocean engineering*, **131(5)**, 239-256.
- [14]Wu, G.X., Ma, Q.W. and Eatock Taylor R. (1998) Numerical simulation of sloshing waves in a 3D tank based on a finite element method. *Applied Ocean Research*, **20(6)**, 337-355.
- [15]Mitra, S., Upadhyay, P.P. and Sinhamahapatra, K.P. (2008) SLOSH dynamics of inviscid fluids in two-dimensional tanks of various geometry using finite element method. *International Journal for Numerical Methods in Fluids*, **56(9)**, 1625-1651.
- [16]Faltinsen, O.M. (1978) A numerical nonlinear method of sloshing in tanks with two-dimensional flow. *Journal of Ship Research*, **22(3)**, 193-202.
- [17]Faltinsen, O.M., Rognebakke, O.F., Lukovsky, I.A. and Timokha, A.N. (2000) Multidimensional modal analysis of nonlinear sloshing in a rectangular tank with finite water depth. *Journal of Fluid Mechanics*, **407**, 201-234.
- [18]Faltinsen, O.M. and Timokha, A.N. (2001) An adaptive multimodal approach to nonlinear sloshing in a rectangular tank. *Journal of Fluid Mechanics*, **432**, 167-200.
- [19]Faltinsen, O.M, and Timokha, A.N. (2010) A multimodal method for liquid sloshing in a two-dimensional circular tank. *Journal of Fluid Mechanics*. **665**, 457-479.
- [20]Liu, D.M., and Lin, P.Z. (2008) A numerical study of three-dimensional liquid sloshing in tanks. *Journal of Computational Physics*, **227(8)**, 3921-3939.
- [21]Veldman, A.E.P., Gerrits, J., Luppens, R., Helder, J.A. and Vreeburg J.P.B. (2007) The numerical simulation of liquid sloshing on board spacecraft. *Journal of Computational Physics*, **224(1)**, 82-99.
- [22]Fang, Z.Y., Duan, M.Y.and Zhu, R.Q. (2007) Numerical simulation of liquid sloshing in a liquid tank based on Level-set method. *Journal of Ship Mechanics*, **11(1)**, 62-67.
- [23]Pan, X.J., Zhang, H.X. and Lu, Y.T. (2008) Numerical simulation of viscous liquid sloshing by moving-particle semi-implicit method. *Journal of Marine Science and Application*, **7(3)**, 184-189.
- [24]Koshizuka, S., Nobe, A. and Oka, Y. (1998) Numerical analysis of breaking waves using the moving particle semi-implicit method. *International Journal For Numerical Methods In Fluids*, **26(7)**, 751-769.
- [25]Gingold, R.A. and Monaghan J.J. (1977) Smoothed particle hydrodynamics-theory and application to non-spherical stars. *Monthly Notices of the Royal Astronomical Society*, **181**, 375-389.
- [26]Lucy, L.B. (1977) A numerical approach to the testing of the fission hypothesis. *The Astronomical Journal*, **82**, 1013-1024.

- [27]Liu, G.R. and Liu, M.B. (2003) Smoothed particle hydrodynamics: a meshfree particle method, World Scientific, Singapore.
- [28]Delorme, L., Iglesias, A.S. and Perez, S.A. (2005) Sloshing loads simulation in LNG tankers with SPH. *International Conference on Computational Methods in Marine Engineering*. Barcelona.
- [29]Iglesias, A.S., Rojas, L.P. and Rodriguez, R.Z. (2004) Simulation of anti-roll tanks and sloshing type problems with smoothed particle hydrodynamics. *Ocean Engineering*, **31(8-9)**, 1169-1192.
- [30]Rhee, S.H. and Engineer, L. (2005) Unstructured grid based Reynolds-averaged Navier-Stokes method for liquid tank sloshing. *Journal of Fluids Engineering*, **127**, 572-582.
- [31]Souto-Iglesias, A., Delorme, L., Perez-Rojas, L. and Abril-Perez, S. (2006) Liquid moment amplitude assessment in sloshing type problems with smooth particle hydrodynamics. *Ocean Engineering*, **33(11-12)**, pp. 1462-1484.
- [32]Anghileri, M., Castelletti, L.M.L. and Tirelli, M. (2005) Fluid structure interaction of water filled tanks during the impact with the ground. *International Journal of Impact Engineering*, **31(3)**,235-254.
- [33]Shao, J.R., Li, H.Q., Liu, G.R. and Liu, M.B. (2012) An improved SPH method for modeling liquid sloshing dynamics. *Computers & Structures*, **100-101**, 18-26.
- [34]Liu, M.B., Shao, J.R. and Chang, J.Z. (2012) On the treatment of solid boundary in smoothed particle hydrodynamics. *Science China*, **55**, 244-254.